Mass and momentum transfer by breaking internal and surface waves in coastal zones

V. Liapidevskii

Lavrentyev Institute of Hydrodynamics, Novosibirsk, Russia

Cowork with:

N. Gavrilov, *LIH, SB RAS, Novosibirsk, Russia ;*

H. Branger, O. Kimmoun, *IRPHE, CNRS, Marseille, France ;*

V. Navrotsky, E. Pavlova, S. Simonenko, *POI, FEB RAS, Vladivostok, Russia .*

- **Internal waves with “trapped” cores**
- **Development of “solibores” over the shelf**
- **Dispersion and mixing effects: mathematical models**

Open question : Waves breaking on a beach : velocity field under the waves ?

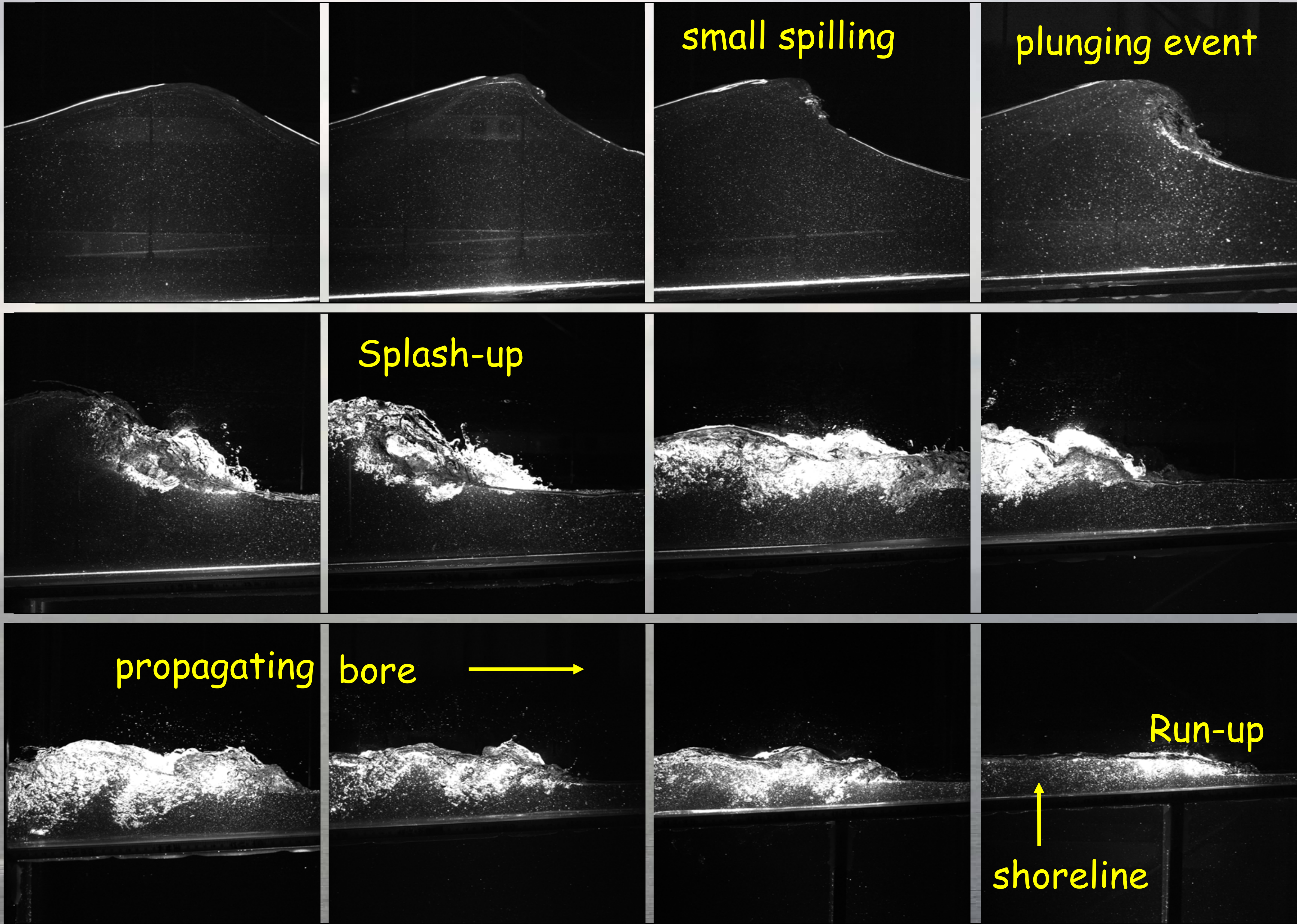
small spilling
plunging event
Splash-up
propagating bore
Run-up
shoreline

Velocity field evolution during run up

(PIV method)

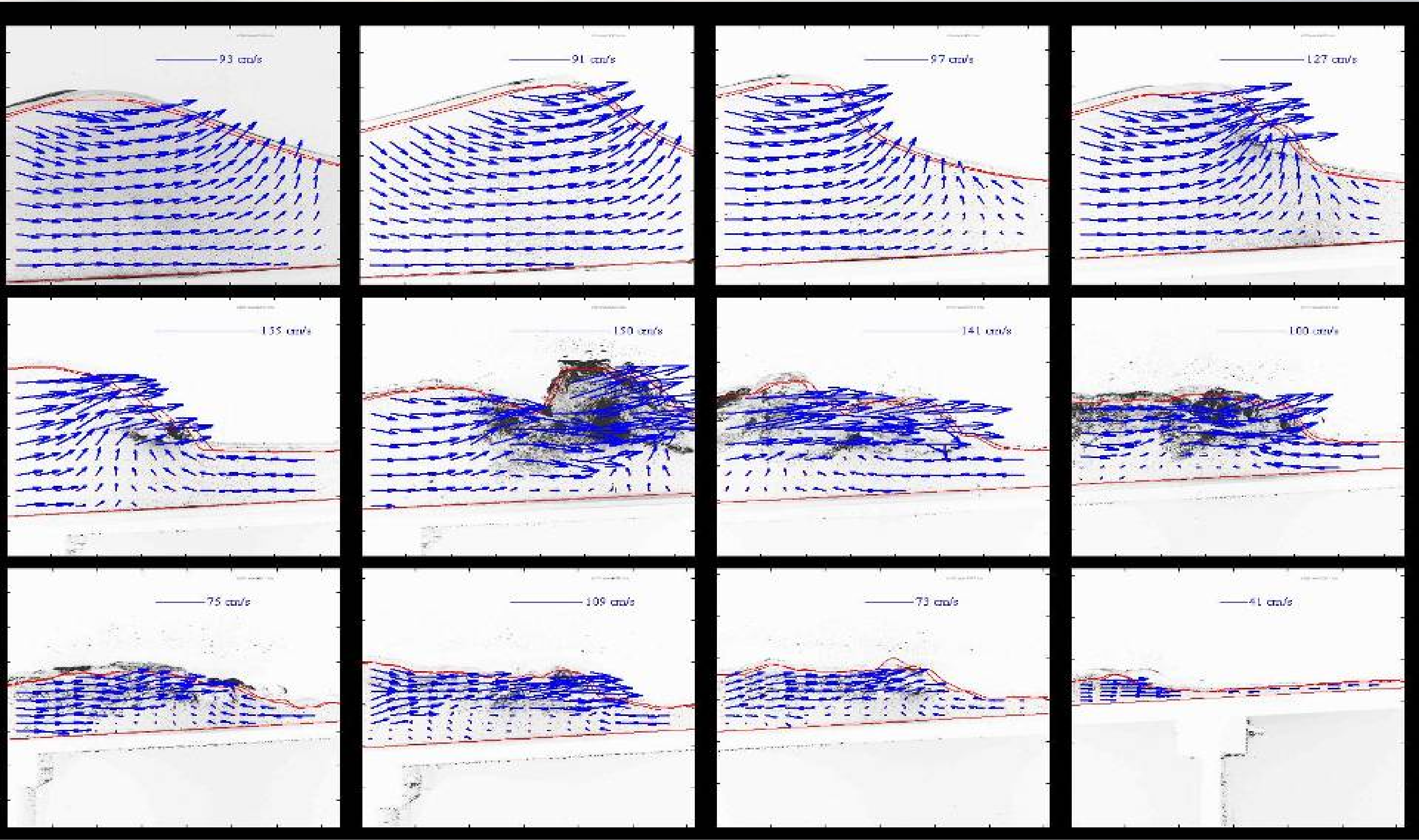

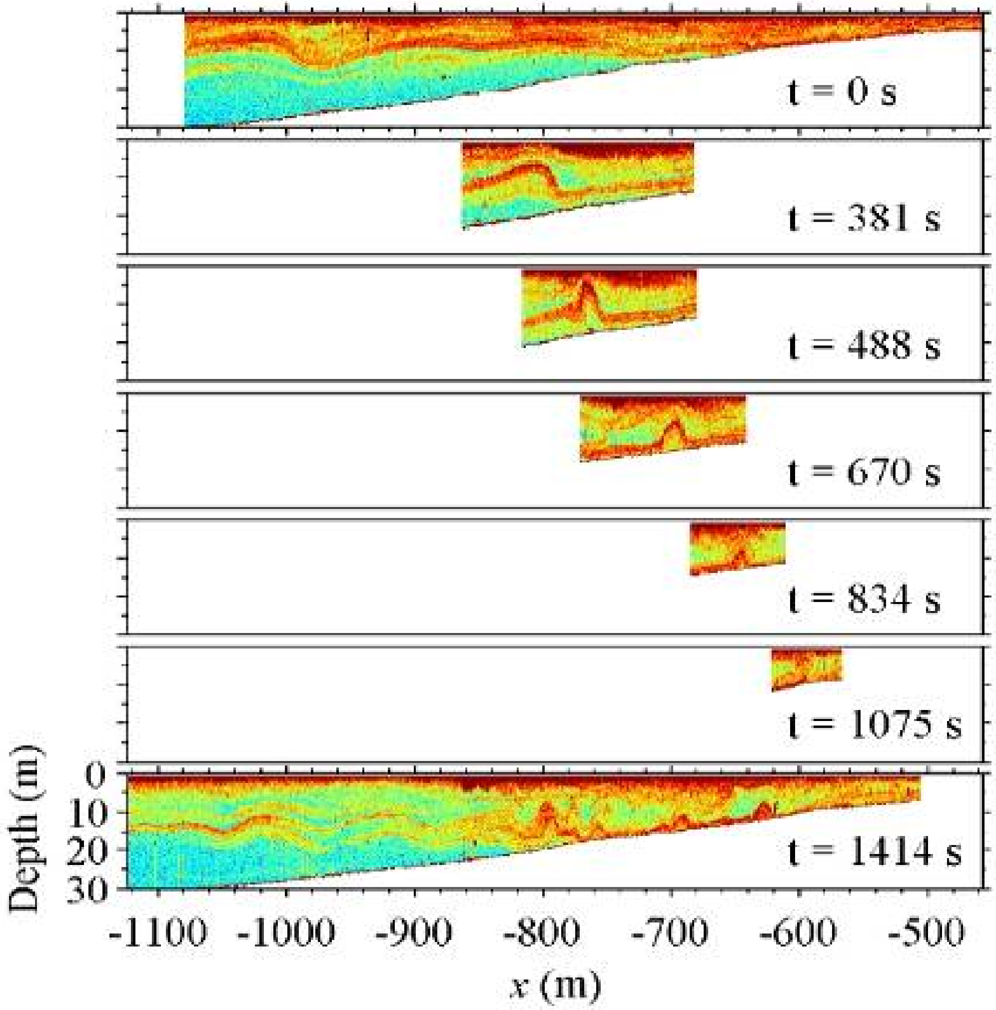

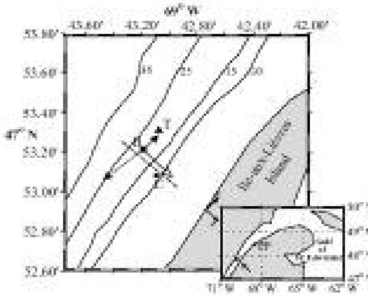

Figure 1. Map of the observational region. The dashed line shows the average transect along which the towed measurements were collected. The axis system used, with x southeastward and y northeastward, is shown with its origin on the edge of the island. The squares mark moorings B and C and the triangle the location of the vertical thermistor chain. The mean surface current is indicated with the solid vector, with the dashed vector representing the mean current below the pycnocline at 13 m depth. The open arrowhead vector indicates the phase speed ($c = 0.6$ m s^{-1}) and direction of the leading wave of the wavetrain (i.e. the wave on the first panel of Figure 3). The reference Pointe-au-Père tidal gauge is marked as PP in the inset.

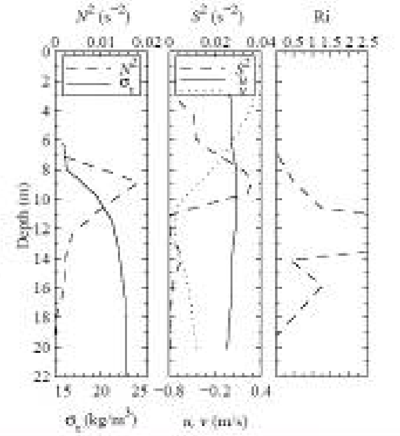

This preprint was prepared with AGU's LaTeX macros v5.01, with the extension package 'AGU++' by P. W. Daly, version 1.5g from 1998/09/14.

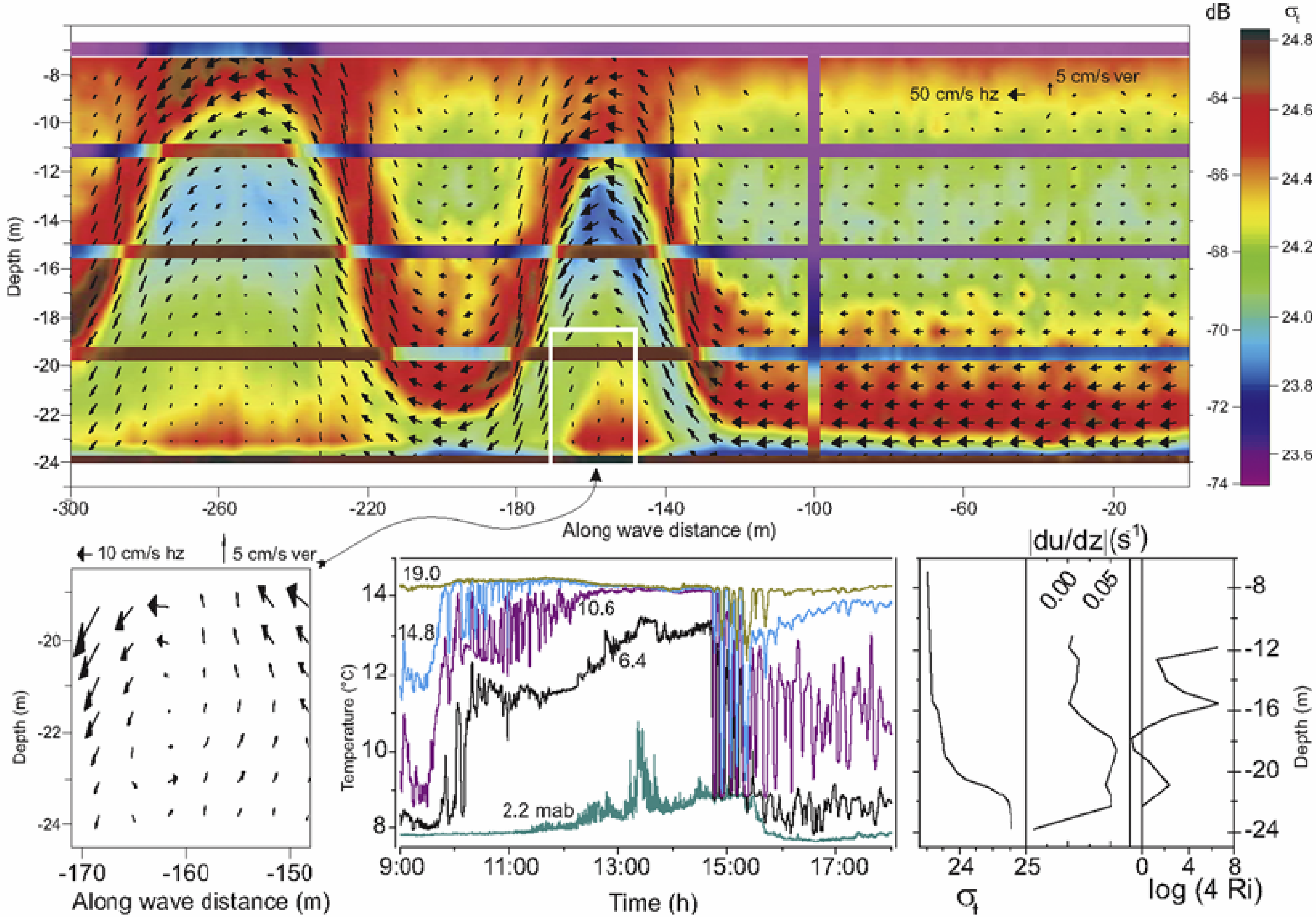

Figure 2. High-frequency internal waves of elevation on 16 September 2001 at A. Top panel. Range-corrected acoustic backscatter intensity from the Acoustic Doppler Current Profiler (background), density record at the depth of the five thermistors (horizontal bars), and current vectors. The time coordinate has been transformed into along-wave distance using the velocity of propagation and currents are shown in a frame of reference moving with the estimated wave speed. The vertical bar at x = −100 m shows the inferred density just ahead of the first wave. The high-backscatter area at the base of the waves marks the extent of the recirculation areas. The white box is magnified in the left bottom panel. Center bottom panel. Temperature record at depths in meters above the bottom over a period of 9 hours. Right bottom panel. Inferred density (left), magnitude of shear (center) and gradient Richardson number (right) just before the arrival of the first wave.

Run up of internal waves

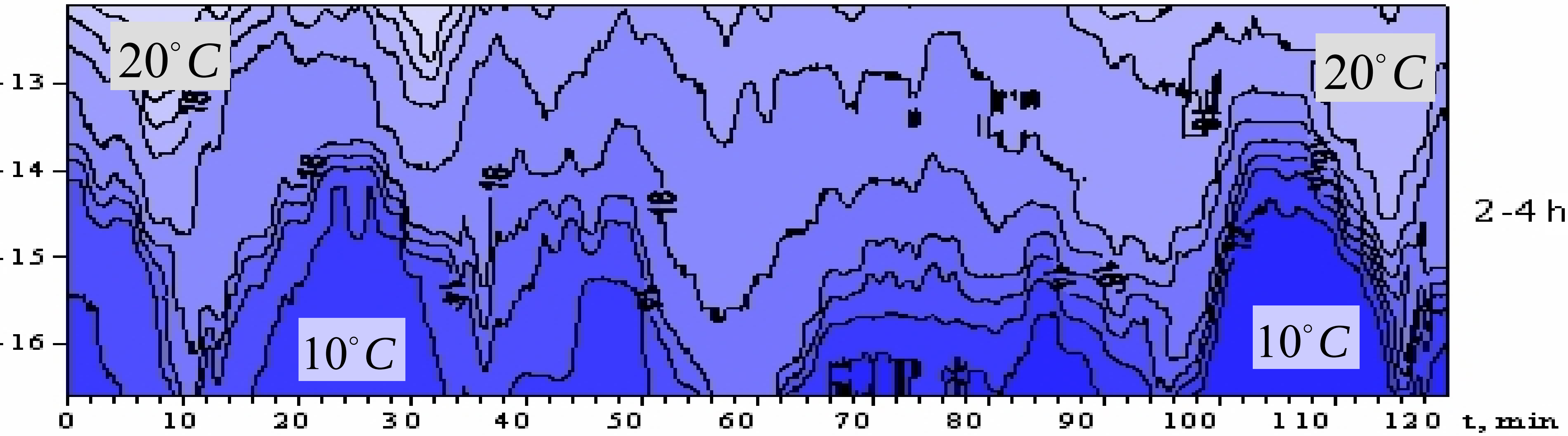

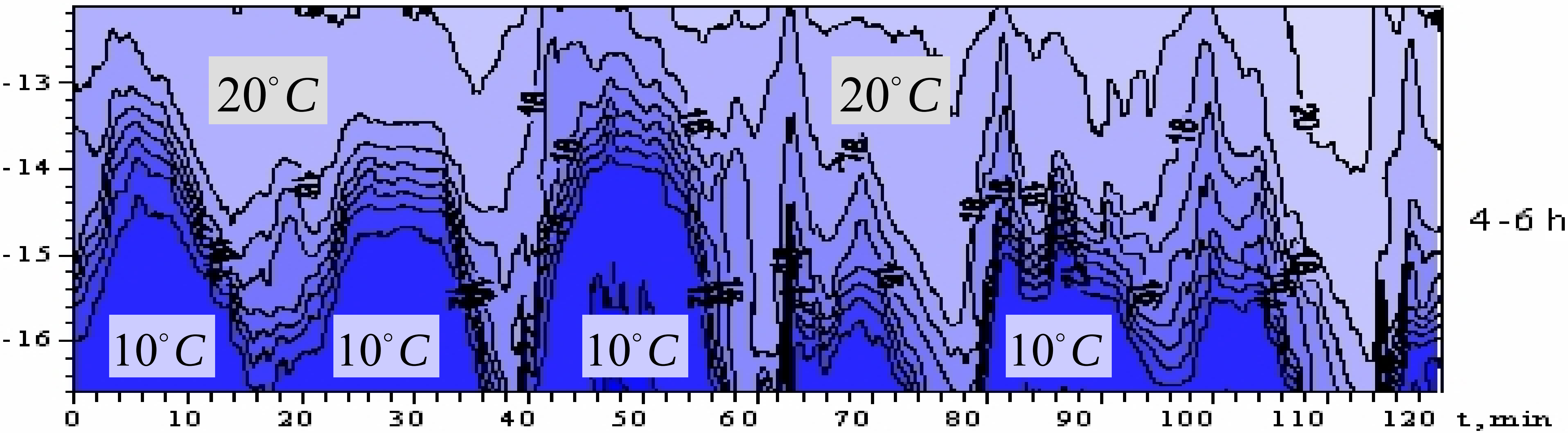

The Sea of Japan, 26.08.2006, the total depth is 16.5 м, the undisturbed depth of thermoclyne is 25 m.

Lock exchange problem for two-layer fluid

Run up over “dry” bottom

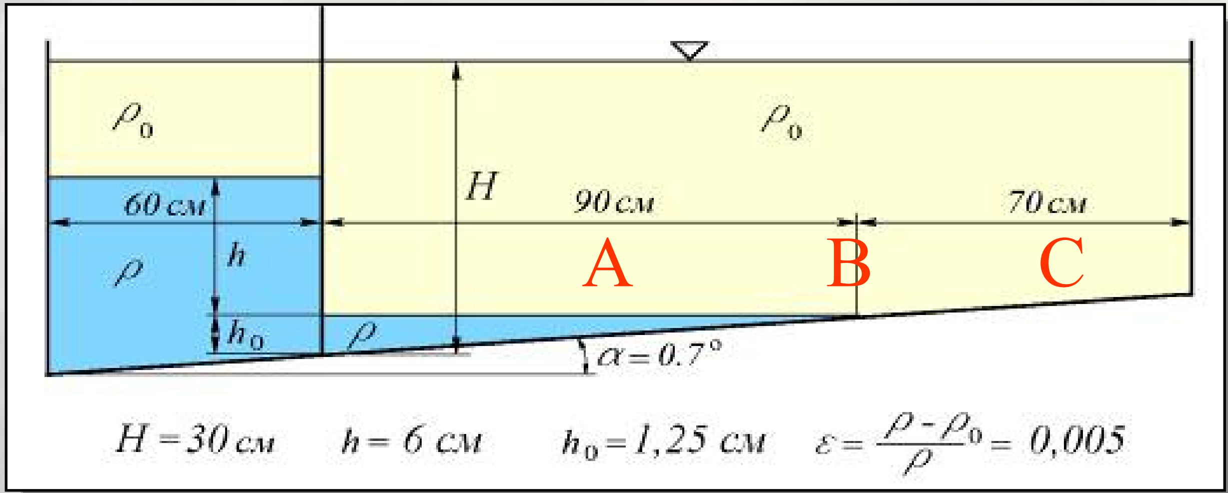

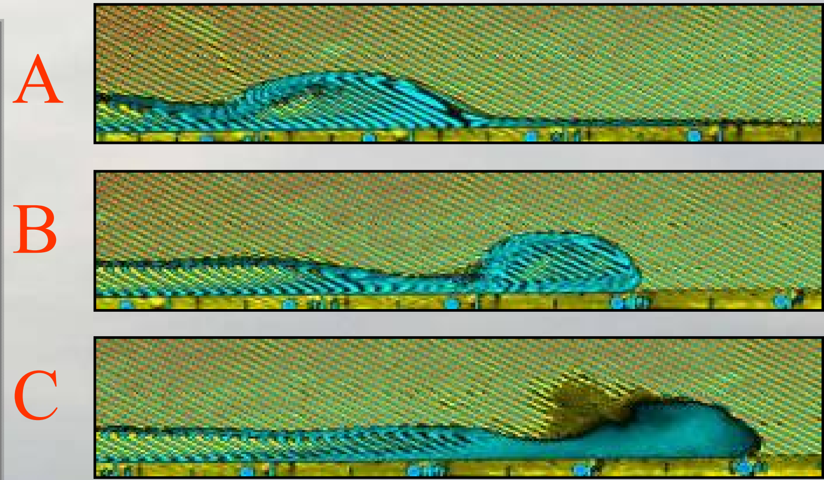

Run up over “wet” bottom

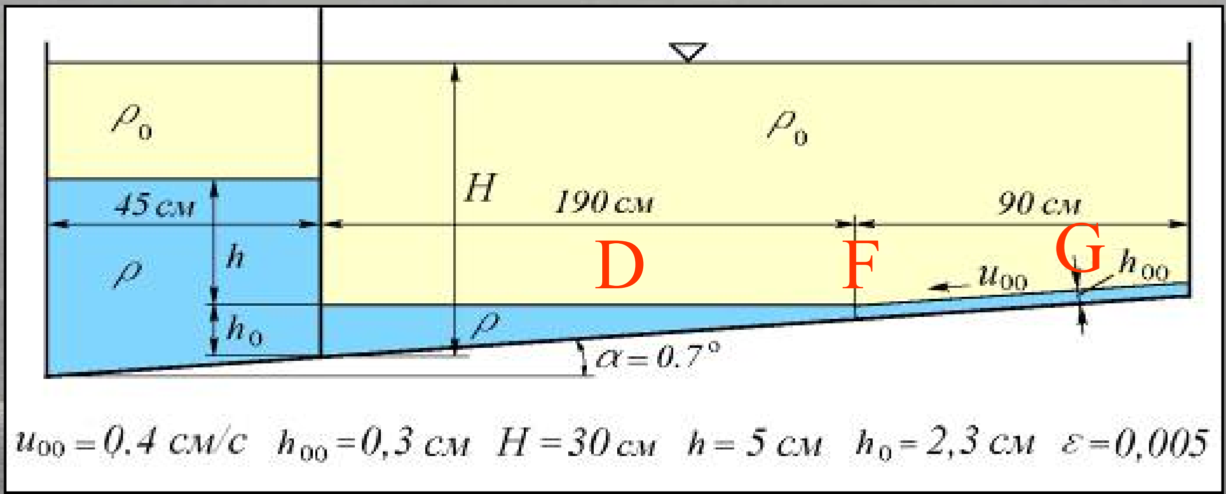

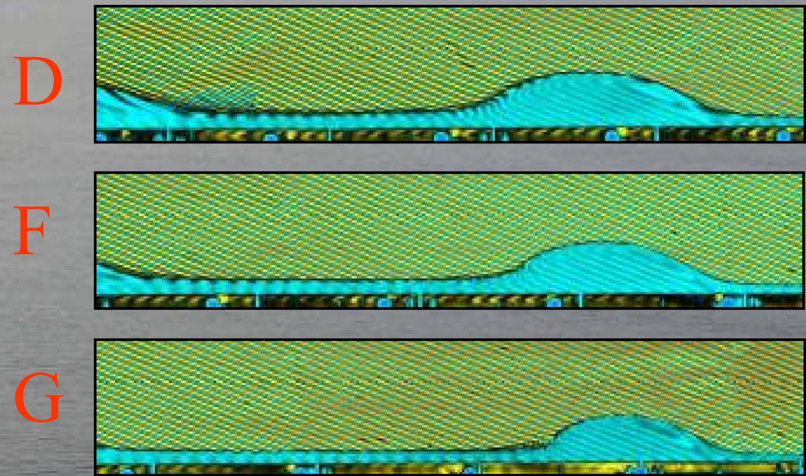

Run up of "solibores" over "dry" and "wet" bottom

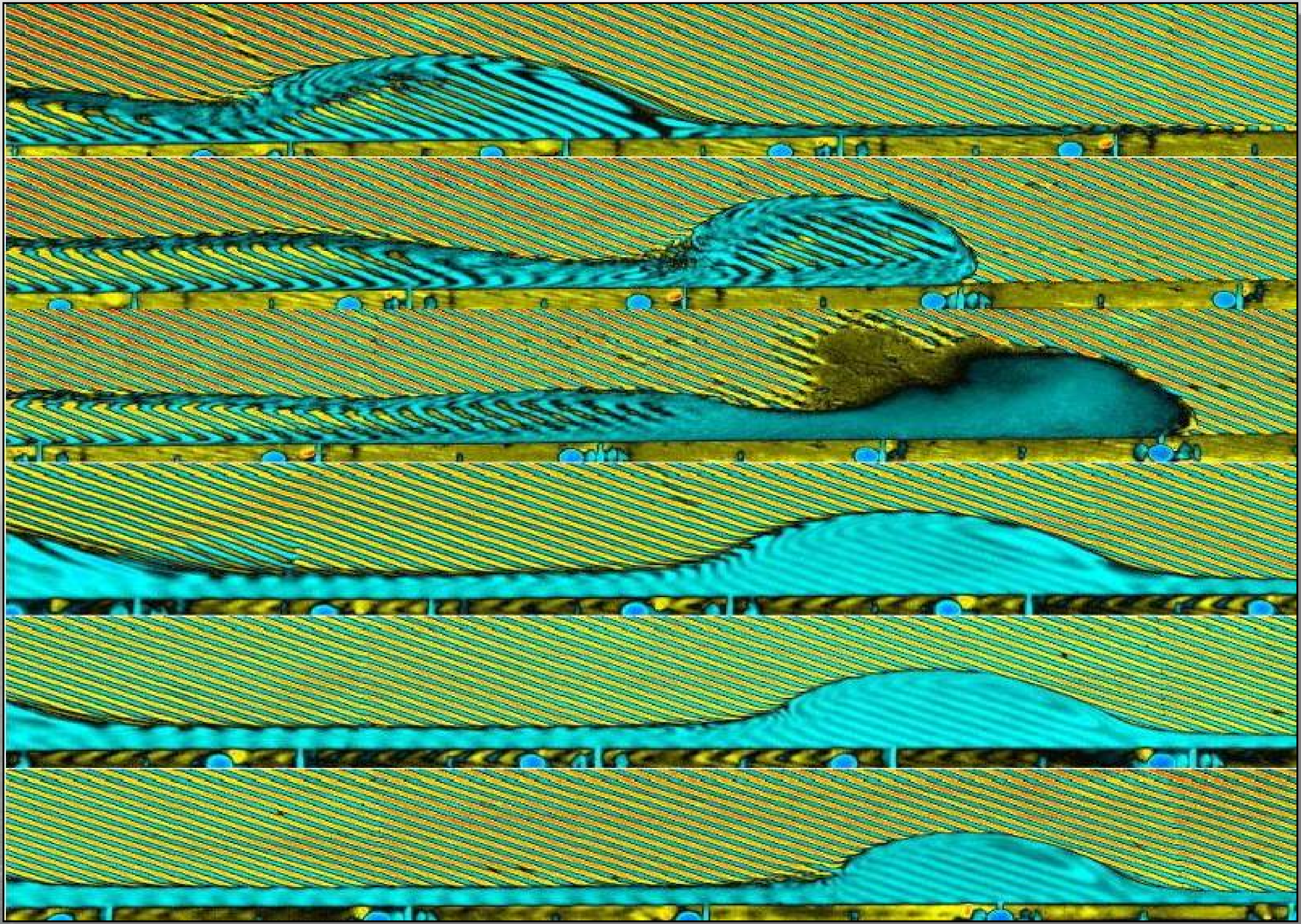

"Solibore" formation

(transition of a wave bore into the gravity flow)

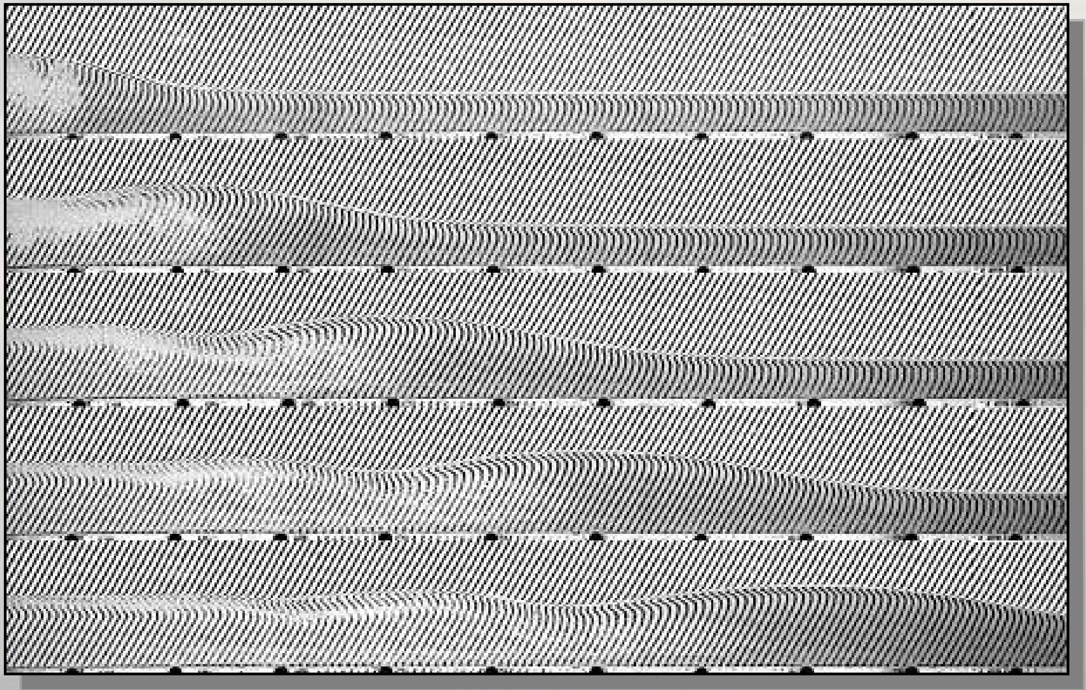

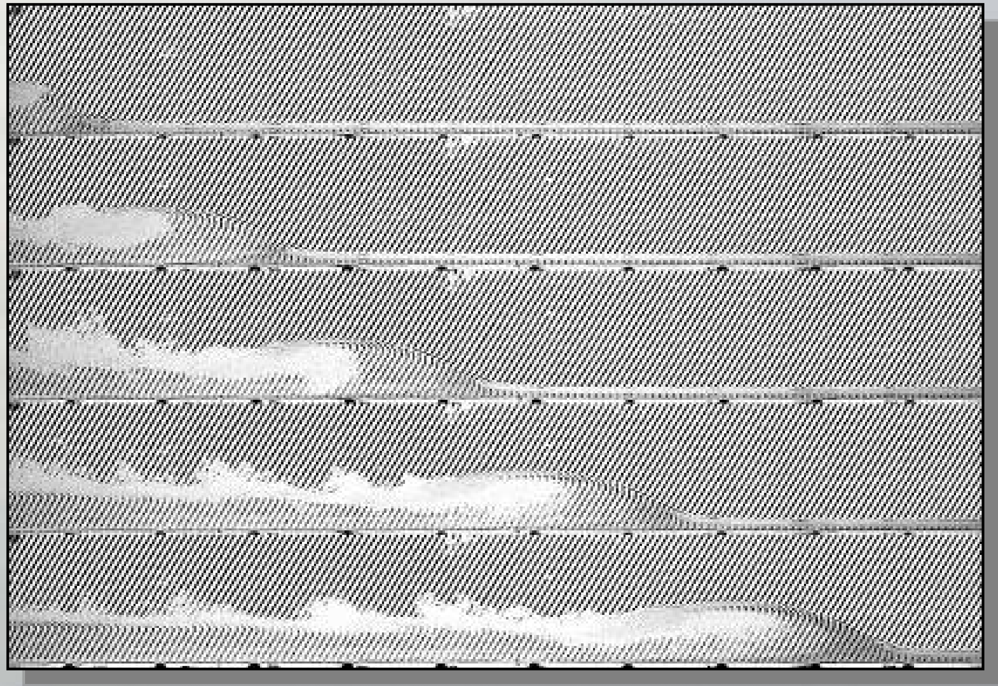

Features of waves with "trapped cores" to be modelled:

• nonhomogeneous velocity distribution at the wave front

• some particles move faster then the wave front

• mixing and entrainment at the interfaces

• dispersion effects

Mathematical model of three-layer flow

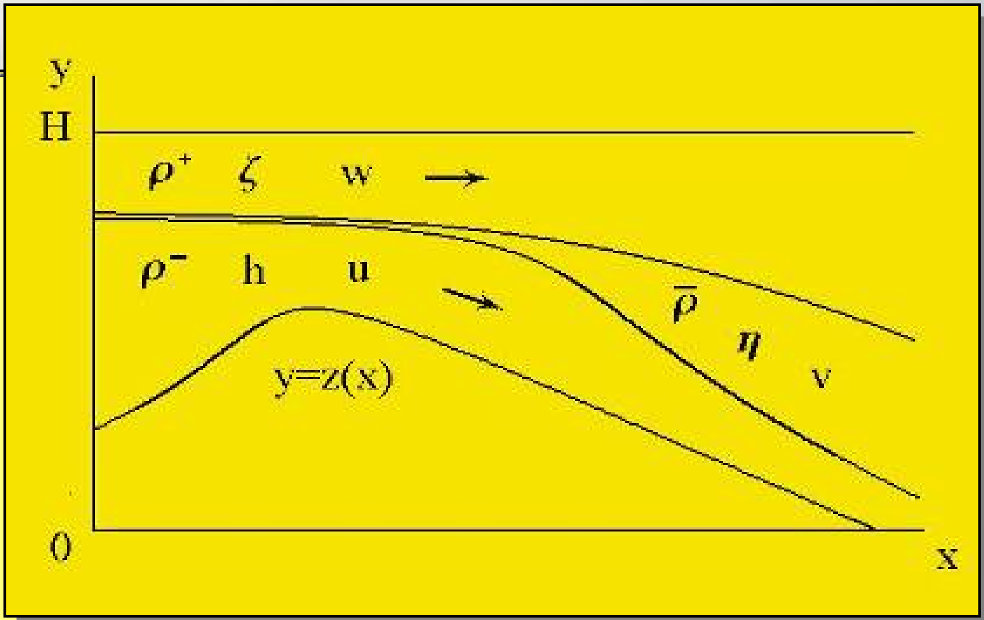

$$h_t + (hu)_x = -\chi^-$$

$$(\zeta)_t + (\zeta w)_x = -\chi^+$$

$$\eta_t + (\eta v)_x = \bar{\chi}$$

$$u_t + \left(\frac{1}{2}u^2 + bh + \bar{b}\eta + p\right)_x = -bz_x$$

$$w_t + \left(\frac{1}{2}w^2 + p\right)_x = 0$$

$$(bh + \bar{b}\eta)_t + (bhu + \bar{b}\eta v)_x = 0$$

$$(hu + \eta v + \zeta w)_t + \Big(hu^2 + \eta v^2 + \zeta w^2 + \frac{1}{2}bh^2 + \bar{b}\eta h + \frac{1}{2}\bar{b}\eta^2 +$$

$$+ (h + \eta + \zeta)p\Big)_x = -(p + bh + \bar{b}\eta)z_x$$

$$(hu^2 + \eta(v^2 + q^2) + \zeta w^2 + bh^2 + 2\bar{b}\eta h + \bar{b}\eta^2)_t +$$

$$+ (hu^3 + \eta v(v^2 + q^2) + \zeta w^3 + 2p(hu + \eta v + \zeta w) + 2\bar{b}\eta hu +$$

$$+ 2\bar{b}(h + \eta)\eta v + 2bh^2 u)_x = -2(bhu + \bar{b}\eta v)\, z_x - \varepsilon$$

Mixing layers and hydraulic jumps in stratified flows

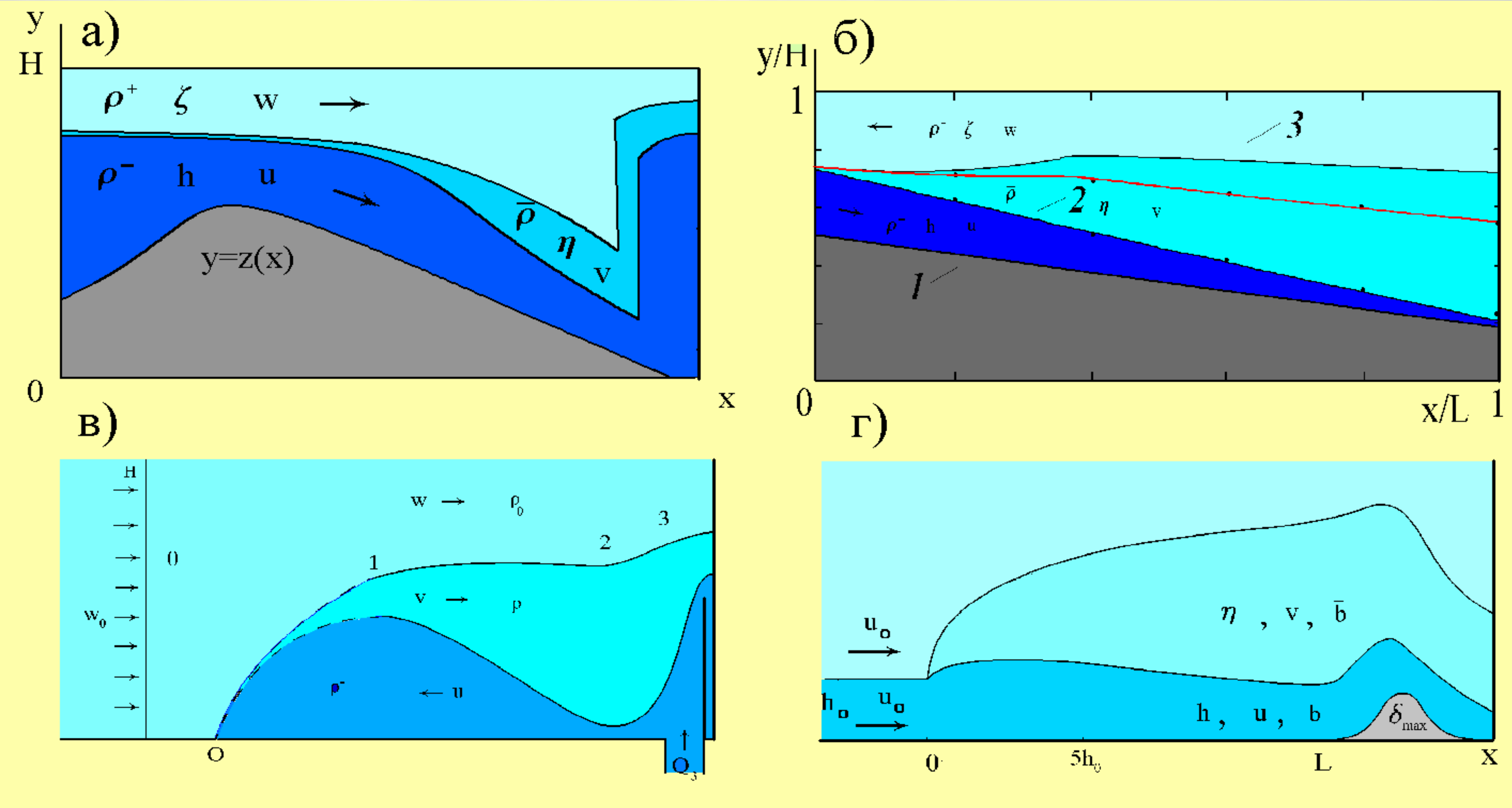

а) lee jump; б) downslope mixing layer; в) gravity current; г) upstream turbulent bore

Mathematical model of spilling breakers in homogeneous fluid

Shallow water equations with surface turbulent layer

$$
\begin{aligned}
&h_t + (hu)_x = -\sigma q,\\
&u_t + uu_x + g(h+\eta+z)_x + p^-_x = 0,\\
&\eta_t + (\eta w)_x = \sigma q,\\
&w_t + ww_x + g(h+\eta+z)_x + p^-_x = \sigma q(u-w)/\eta,\\
&q_t + wq_x = \sigma((u-w)^2 - q^2)/(2\eta),\\
&\sigma = 0.15, \qquad z = z(x) \ - \ \text{bottom form}
\end{aligned}
$$

$$
\begin{aligned}
&a) \quad p = gh \qquad \left(p^- = 0\right)\\
&b) \quad p = p(h, dh/dt, d^2h/dt^2)\\
&c) \quad p = p(h, d\tilde{h}/dt, d^2\tilde{h}/dt^2)
\end{aligned}
$$

a) hydrostatic model;

b) dispersive model;

c) hyperbolic model.

Turbulent bores in homogeneous fluid

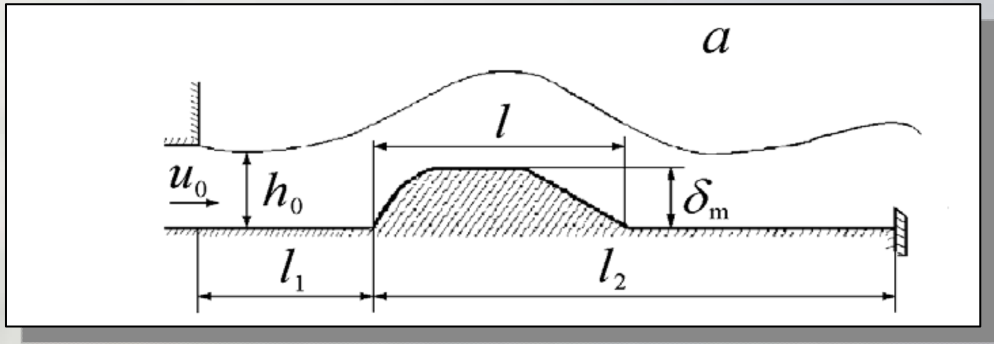

Bold points: experiment by V. Bukreev (Fr = 2.9),

Thick lines: hydrostatic model of breaking waves.

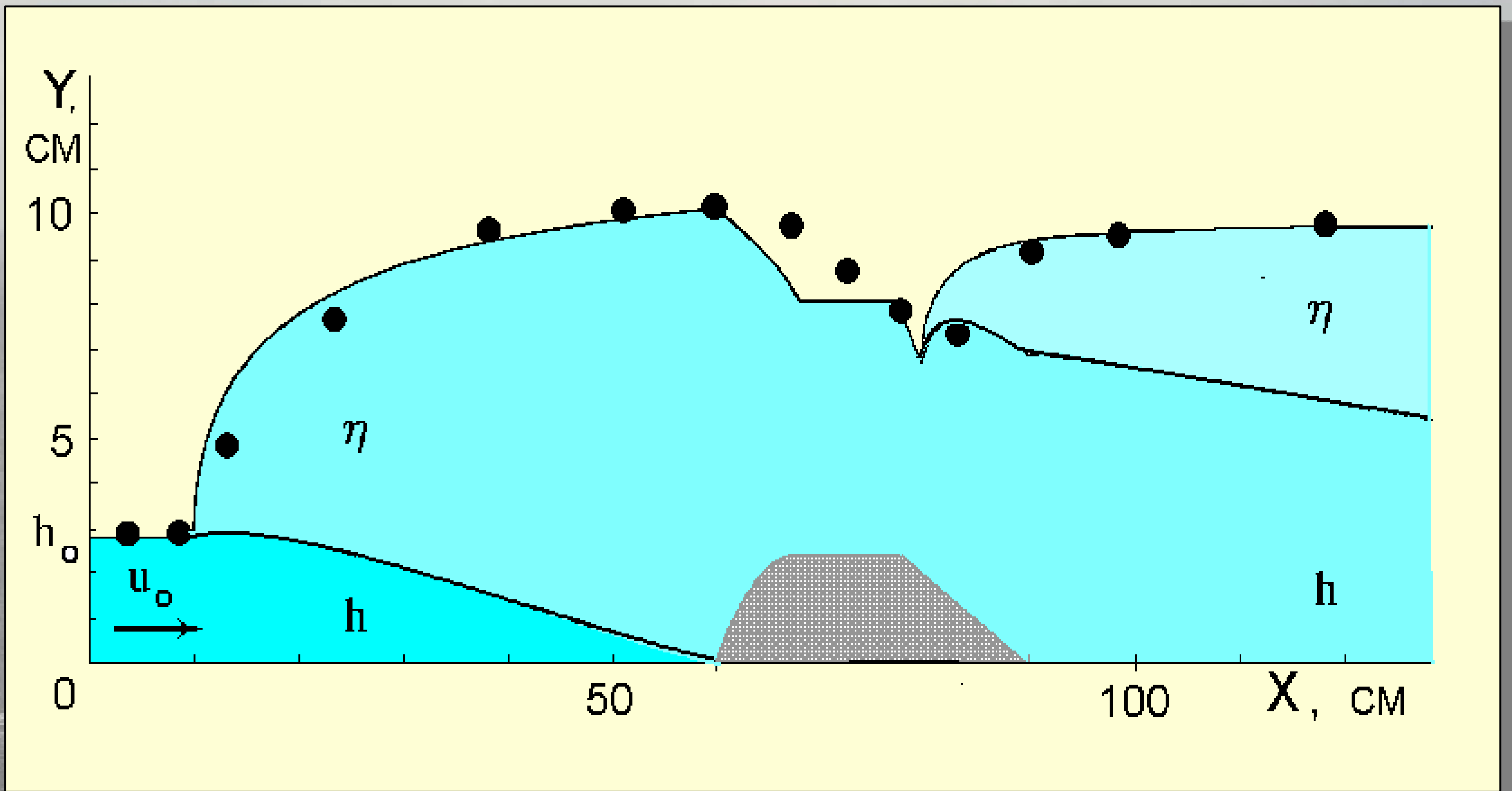

Turbulent bores development

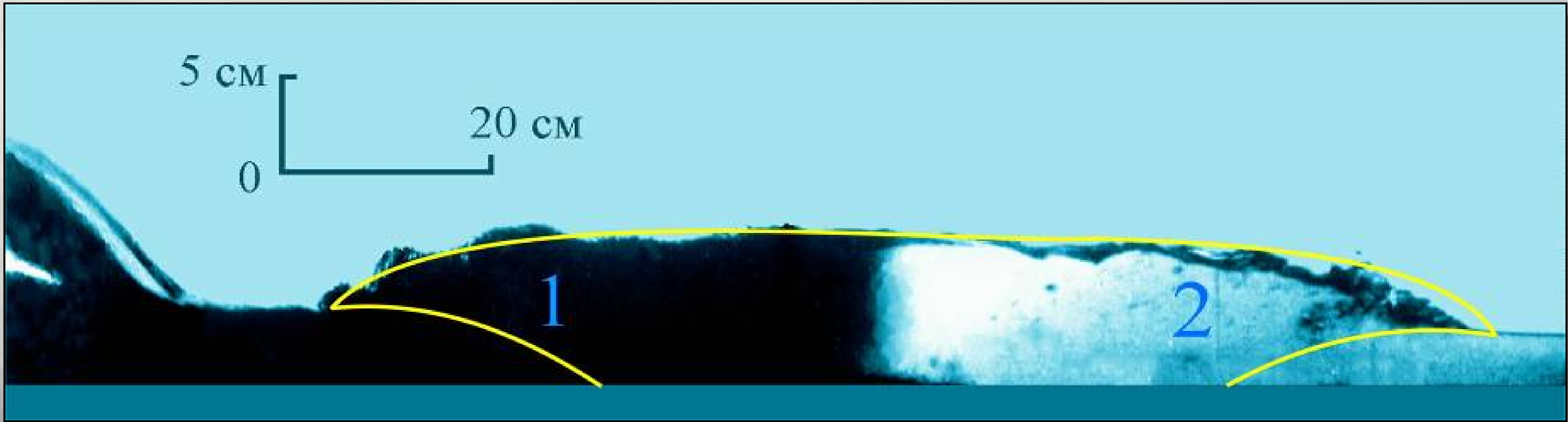

Nonstationary surface wave configuration, consisting of the two turbulent bores moving with different velocities: *1*, *2* – the free surface and the lower boudary of the turbulent layers (yellow line: nonstationary calculation by the hydrostatic model)

Conclusions

Laboratory experiments

Common features of the transition from an undular bore to the spilling breaker in homogeneous and stratified fluids:

- “trapped core” formation
- particles move faster the wave front
- entrainment and turbulent mixing

Mathematical models

- Two-layer scheme of flow with turbulent mixing layer gives the adequate description of the spilling breaker structure
- The shallow water equations taken into account the mixing and dispersion effects give the criterion of transition from smooth waves to breaking waves